ACS APPLIED ENERGY MATERIALS

www.acsaem.org Letter

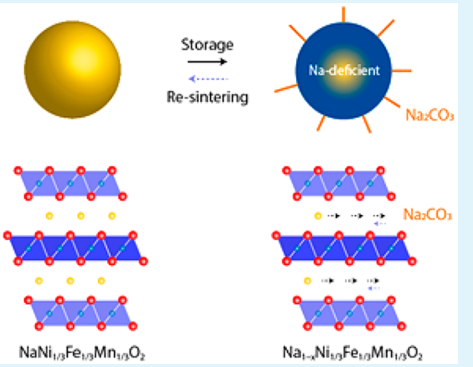
Degradation Mechanism of O3-Type $NaNi_{1/3}Fe_{1/3}Mn_{1/3}O_2$ Cathode Materials During Ambient Storage and Their In Situ Regeneration

Yang Sun, Hong Wang,* Dechao Meng, Xiaoqiao Li, Xiaozhen Liao, Haiying Che, Guijia Cui, Fengping Yu, Weimin Yang, Linsen Li,* and Zi-Feng Ma*

Cite This: https://dx.doi.org/10.1021/acsaem.1c00047 Read Online

ACCESS | Metrics & More | Article Recommendations | Supporting Information

ABSTRACT: Sodium-ion batteries (SIBs) hold great promise for low-cost energy storage. Despite the major advances made in the material preparation and battery performance, air instability has become a bottleneck for the storage and electrode fabrication of O3-type $NaNi_{1/3}Fe_{1/3}Mn_{1/3}O_2$ (NFM), but the underlying mechanism remains elusive. Here we discovered that NFM loses Na^+ ions during ambient storage and Na_2CO_3 "fibers" sprout from the particle surface, which caused the performance decay. We further demonstrated a facile resintering strategy to regenerate the NFM *in situ*. This work highlights the importance of stringent humidity control and provides the basis for designing surface-modification strategies.



KEYWORDS: *air instability, cathode materials, sodium-ion batteries, regeneration, degradation mechanism, correlative SEM-Raman*

Downloaded via SHANGHAI JIAO TONG UNIV on March 17, 2021 at 07:58:55 (UTC).
See https://pubs.acs.org/sharingguidelines for options on how to legitimately share published articles.

Sodium-ion batteries (SIBs) have attracted significant interest in recent years because they operate similarly to lithium-ion batteries (LIBs) but may potentially cost much less thanks to the abundance of sodium (Na) versus lithium (Li) and the substitution of copper by aluminum as anode current-collector.[1−3] In SIBs, the cathode materials play a crucial role because their physiochemical and electrochemical properties directly impact the battery-level energy density, power capability, and safety. Numerous cathode materials have been studied, including layered oxides,[4−7] Prussian-blue analogues,[8,9] and polyanion-based compounds,[10,11] among which the O3-type layered oxides stand out because of their high specific capacity, good cycle performance, and facile preparation methods.[12,13] G. Ceder et al. reported O3-$NaNi_{1/3}Fe_{1/3}Co_{1/3}O_2$ that exhibited a discharge capacity of 165 mAh g^{-1} at 0.05 C in 4.2−2.0 V.[14] Y. Hu et al. reported O3-$Na_{0.9}[Cu_{0.22}Fe_{0.30}Mn_{0.48}]O_2$ that provided a reversible capacity of ∼100 mAh g^{-1} at an average voltage of 3.2 V and good cycle performance.[15] C. Johnson et al. first reported O3-$NaNi_{1/3}Fe_{1/3}Mn_{1/3}O_2$ (NFM), which retained a specific capacity of 100 mAh g^{-1} after 150 cycles in half-cell tests.[16] NFM is free of cobalt, an expensive metal (∼$30000−40000 per metric ton) with an unstable supply chain. Instead, NFM is made of earth-abundant iron (Fe) and manganese (Mn) and thus has a cost advantage over many other Na cathode materials. Our research group has focused our efforts on NFM over the years and studied its large-scale synthesis,[17] electrochemical reaction mechanism,[18] and thermal stability.[19] In particular, by optimizing the microstructure of NFM and electrolyte engineering,[20] it is now possible to achieve a cycle-life over 2500 cycles in 1 Ah pouch cells (NFM-hard carbon) and a specific energy density of ∼105 Wh kg^{-1} at the single-cell level.[21] These attributes have established NFM as a practically relevant cathode material for SIBs.

Despite the progress achieved in the electrochemical performance of NFM, we have noticed slurry alkalization and "gelling" during the fabrication of NFM electrodes under ambient conditions in air (∼40% relative humidity, RH). This observation suggests that NFM is likely susceptible to degradations upon air exposure, which is a common problem facing Ni-rich or Li-rich transition metal oxides for LIBs as well.[22,23] Recently, Y. Yang et al. studied the structural/chemical transformations of P2-type sodium transition metal oxides upon contact with moist air; these materials were found to suffer from hydration (H_2O intercalating into the layered structure) during storage.[24] A. Manthiram et al. studied the degradation chemistry of a high-Ni Na cathode (O3-type $NaNi_{0.7}Co_{0.15}Mn_{0.15}O_2$) in air and observed the rapid formation of NaOH, Na_2CO_3, $Na_2CO_3{\cdot}H_2O$, and NiO on the particle surface (within hours) that caused a significant

Received: January 6, 2021
Accepted: March 1, 2021

© XXXX American Chemical Society

https://dx.doi.org/10.1021/acsaem.1c00047
ACS Appl. Energy Mater. XXXX, XXX, XXX−XXX

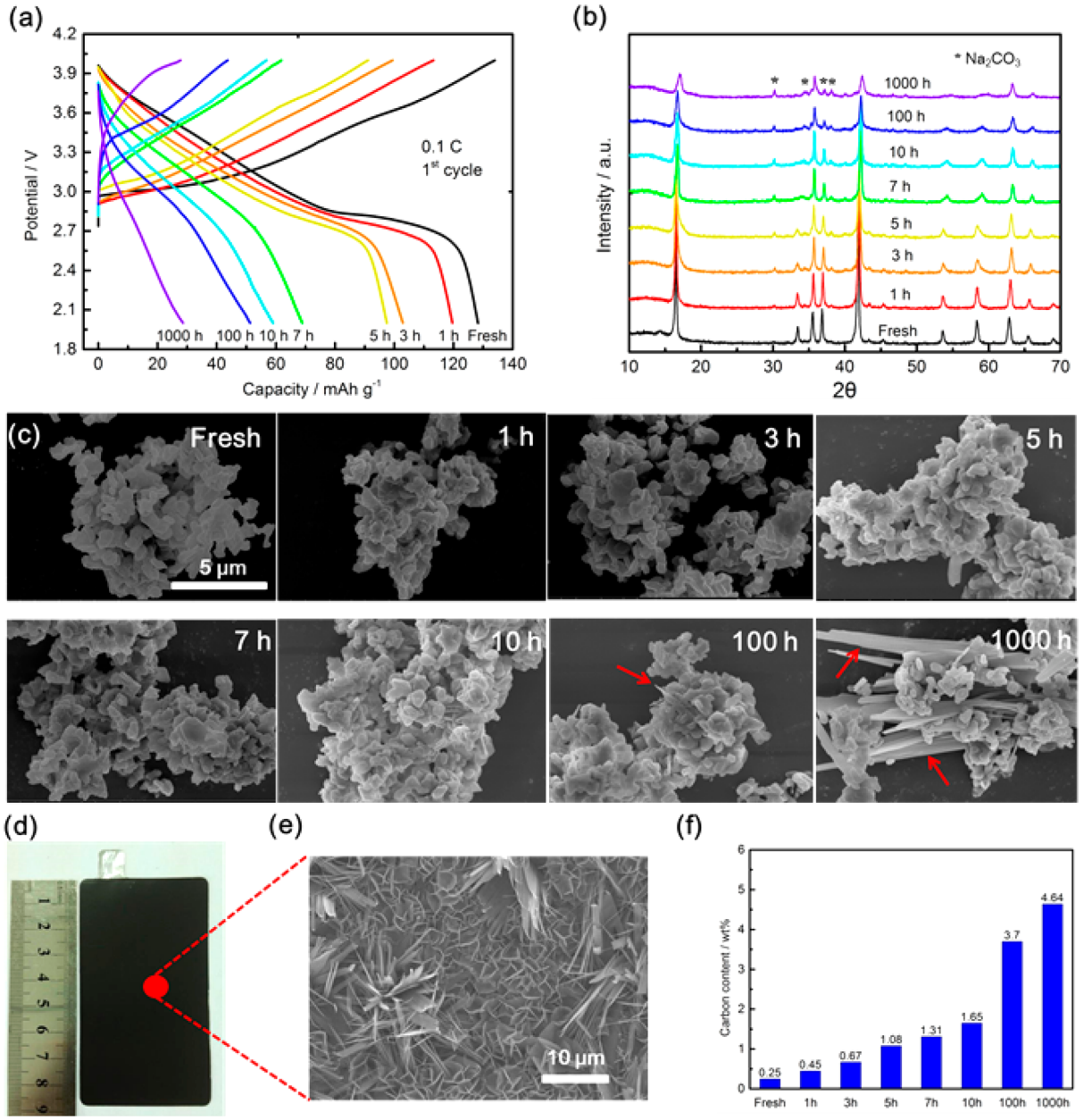


Figure 1. $NaNi_{1/3}Fe_{1/3}Mn_{1/3}O_2$ cathode materials after ambient storage: (a, b) the first discharge voltage profiles and XRD patterns of the NFM samples as a function of storage time under ambient conditions, respectively; (c) SEM images of the aged NFM showing the gradual formation of fiber-like particles at the surface as indicated by the red arrows; (d) an NFM electrode used for pouch-cell assembly and tests, which had been stored under ambient conditions for ~1000 h; (e) SEM image taken from the electrode sheet in panel d showing the rampant growth of fiber-like particles; and (f) elemental analysis of the carbon content in the NFM samples as a function of storage time.

electrochemical performance decline.[25] It appears that the degradation mechanism of different cathode materials depends on the composition and crystal structure.[26−28] To facilitate the large-scale production of NFM-based SIBs, it is necessary to elucidate the degradation mechanism of NFM during ambient storage, which is pivotal in designing improvement strategies. The research efforts along this direction are currently lacking.

Here we investigated the degradation mechanism of NFM under ambient storage (up to 1000 h) and revealed the structural origins of electrochemical performance decay. We combined a suite of characterization techniques to study the morphological, chemical, and structural transformations of the NFM during storage. It was found that NFM became Na-deficient after the storage, and the "lost" Na reacted with CO_2 to produce Na_2CO_3 at the particle surface; this was responsible for the significant capacity loss. Further, we found that high-performance NFM could be regenerated *in situ* by directly sintering the degraded NFM and the "byproduct" (Na_2CO_3) at high temperature. This work unlocks the nature of air instability of NFM and lays the foundation for improving air-sensitive Na cathode materials toward practical applications.

The fresh NFM material was synthesized by sintering the coprecipitated $Ni_{1/3}Fe_{1/3}Mn_{1/3}(OH)_2$ and Na_2CO_3 at 850 °C in air following a previously reported method[17] (also see Experimental Methods in the Supporting Information). We first evaluated the impact of storage time on the electrochemical performance of NFM. The NFM powders were stored in ambient air (RH = ~40−50%) for different amount

https://dx.doi.org/10.1021/acsaem.1c00047
ACS Appl. Energy Mater. XXXX, XXX, XXX−XXX

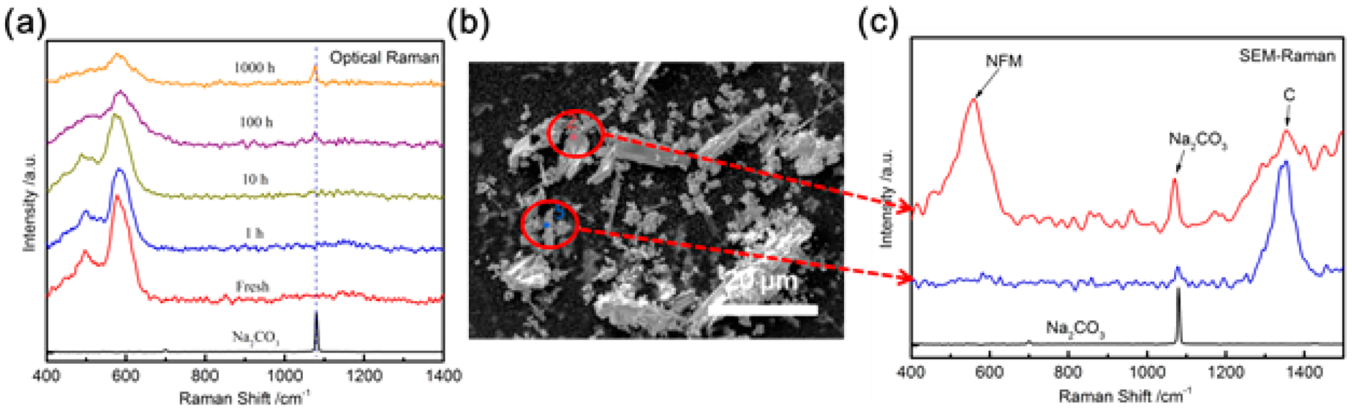


Figure 2. (a) Raman spectra of the NFM samples after ambient storage for a different amount of time. (b) SEM image of the NFM particles supported on a carbon tape after 1000 h of storage. (c) Single-point Raman spectra were collected from two locations where fiber-like particles could be seen, as indicated by the red circles. A strong signal at ∼1077 cm^{-1} was observed, matching the characteristic peak in the Na_2CO_3 reference.

of time, then made into electrodes, and tested in half cells using Na metal as the anode. Figure 1a shows the voltage curves of the aged NFM electrodes at the first discharge. The specific capacities decreased as the storage time increased; these were 130 (fresh, 0 h), 120 (1 h), 103 (3 h), 94 (5 h), 69 (7 h), 58 (10 h), 51 (100 h), and 28 mAh g^{-1} (1000 h), respectively. The polarization also increased with the storage time. The degraded electrochemical performance suggested that significant structural/chemical transformations had happened to the NFM material during storage.

To understand the structural origins of the performance decay after storage, we first collected powder X-ray diffraction (XRD) patterns from the fresh and aged NFM powders (Figure 1b). The freshly prepared NFM sample could be indexed to a single phase with an α-$NaFeO_2$-type structure. As the storage time increased, the characteristic peaks of NFM remained, but their intensity decreased, indicative of structural transformations. We also observed that several new peaks emerged after just 1 h of storage, and their intensity increased with the storage time (denoted by * in Figure 1b). These peaks appear to match well with those of Na_2CO_3. We further studied the variation of the interlayer spacing among the fresh, aged, and regenerated NFM materials. We collected high-resolution PXRD patterns from the three samples and carried out the Rietveld refinements for the fresh and regenerated NFM materials (Figure S1). The aged NFM sample contained Na_2CO_3 and showed a poor signal-to-noise ratio compared with the other patterns. We were not able to do refinements but chose to estimate the interlayer spacing based on the 2θ angle of the (003) peak using the Bragg equation. The lattice parameter c was determined to be 15.981, 16.022, and 15.997 Å for the fresh, aged, and regenerated NFM materials.

Scanning electron microscopy (SEM) characterizations were performed to understand the morphological evolution of the NFM particles during storage (Figure 1c). The freshly prepared NFM consisted of nanoparticle aggregates with smooth surfaces. With an increase in storage time, we observed changes at the surface of the primary particles and also between neighboring particles. The particle surface was no longer smooth. After 100 h, some fiber-like particles were observed to sprout out from the NFM particles (indicated by a red arrow in Figure 1c). After 1000 h, a significant amount of fiber-like particles were present in the sample. In the NFM electrode used for the pouch-cell assembly (Figure 1d), we observed even more rampant growth of fibers at the electrode surface after ∼1000 h of storage (Figure 1e). Elemental analysis also showed an increase in the carbon content as a function of storage time (Figure 1f).

We further carried out optical Raman spectroscopy measurements to study the structural changes in the NFM samples to complement the results from XRD, SEM, and elemental analysis. Figure 2a shows the Raman spectrum collected from the aged NFM samples in comparison with a reference spectrum of Na_2CO_3. Two characteristic peaks were observed for the freshly prepared NFM at ∼496 and 578 cm^{-1}, which can be attributed to Ni−O and Mn−O stretching.[23] The peaks became weaker and broader with an increase in storage time, which was indicative of a less ordered structure. In addition, a new peak appeared at ∼1077 cm^{-1} after 10 h, and its intensity continued to grow with the storage time. These results further supported the presence of Na_2CO_3 in the aged NFM samples after ambient storage and made us wonder if the fiber-like particles observed by SEM (Figure 1c) were actually Na_2CO_3.

To identify the composition of the fiber-like particles, we carried out correlative SEM-Raman studies on the NFM sample stored for 1000 h. The measurements were made in an SEM integrated with a Raman microscope, which enables high-resolution morphological information and spatially resolved structural information. Figure 2b shows the SEM image of the aged NFM particles loaded at the surface of a piece of carbon tape. We collected single-point Raman spectra from two locations where the fiber-like particles were visible and indeed observed strong signals at the position that matched well with the Na_2CO_3 reference (Figure 2c).

The air instability of the O3-type NFM material is similar to those of $NaNi_{0.7}Mn_{0.15}Co_{0.15}O_2$[25] and $NaNi_{1/3}Mn_{1/3}Co_{1/3}O_2$[27] but is in striking contrast with those of its Li counterparts. Little change in surface chemistry and particle morphology was observed for Li-NMC111 even after ambient storage for 1 year.[23] In the case of a Ni-rich NMC such as $LiNi_{0.8}Mn_{0.1}Co_{0.1}O_2$ (Li-NMC811), which is considered to be more sensitive to moist air, a surface layer mostly composed of nickel carbonate species mixed with minor quantities of hydroxide and water was formed and caused a significant performance decay.[23] NFM appeared to be more reactive toward CO_2 as more carbonates were formed in a much shorter time (4.64 wt % after 1000 h, Figure 1f) compared with Li-NMC811 (0.39

https://dx.doi.org/10.1021/acsaem.1c00047
ACS Appl. Energy Mater. XXXX, XXX, XXX−XXX

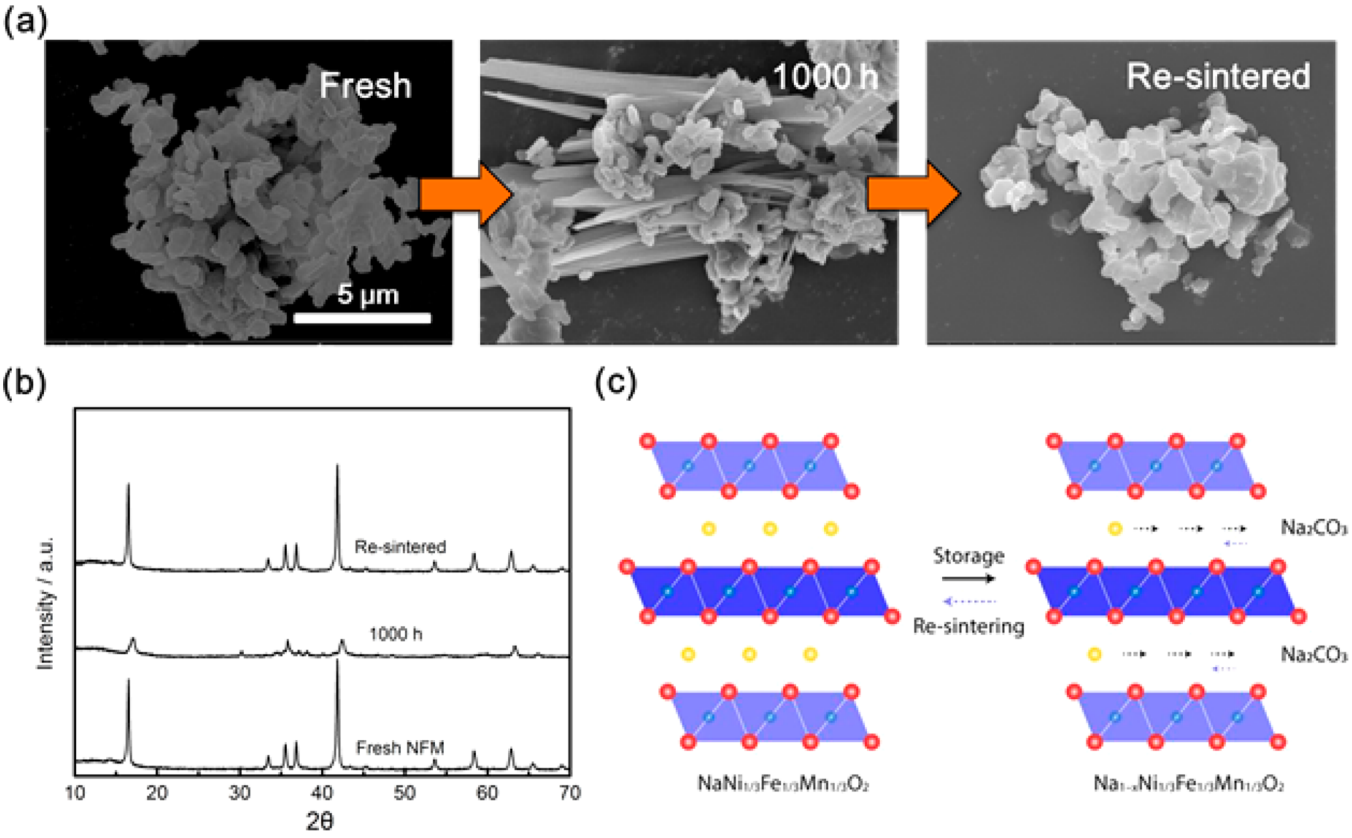


Figure 3. Regeneration of the degraded $NaNi_{1/3}Fe_{1/3}Mn_{1/3}O_2$. (a) SEM images of freshly prepared, 1000 h stored, and resintered NFM particles. Fiber-like Na_2CO_3 particles were formed during storage but disappeared after resintering. (b) XRD patterns of the three samples showing that the crystal structure of NFM could be restored after resintering; (c) Schematic illustration of the structural evolution during storage and resintering.

wt % after 1 year).[23] NFM was also much more reactive toward H_2O and suffered a significant loss of Na after immersion in H_2O (~8% Na remaining after 24 h soaking according to ICP-AES). By contrast, water-washing is now a procedure commonly adopted in the Ni-rich Li-NMC manufacturing industry to control the surface pH (i.e., basicity) and shows little negative impact on the bulk structure and electrochemical performance of the Li-NMC material.[29] The difference in reactivity toward CO_2 or H_2O between the O3-type Na cathode material and its Li counterparts may be understood in terms of ion migrations in the two host lattices. In Li-NMC, the transition metal (TM) ions are known to migrate to the Li sites, producing a cation-mixing surface layer that is less permeable to Li^+ to provide self-passivation.[22] Due to the larger ionic radius of Na^+ (1.02 Å) versus Li^+ (0.76 Å) and thus a larger mismatch between the Na^+ and TM ions (e.g., 0.69 Å for Ni^{2+}), it is more difficult to have TM migration to the Na sites to activate the self-protection. The O3-type Na cathode materials face a serious challenge during storage and fabrication of electrodes, similar to Ni-rich Li-NMCs such as $LiNi_{0.8}Mn_{0.1}Co_{0.1}O_2$ and $LiNi_{0.83}Mn_{0.05}Co_{0.12}O_2$. Stringent humidity control, which is currently applied to Ni-rich Li-NMCs, will be indispensable throughout the material production and processing processes of O3-type Na cathodes to ensure good electrochemical performance.

It is now clear that the NFM material loses Na and Na_2CO_3 is formed at the surface after ambient storage. Since Na_2CO_3 is a precursor for the synthesis of NFM and the fiber-like Na_2CO_3 particles appeared to be homogeneously mixed with the degraded NFM particles (Figures 1c and 3a, after 1000 h), it is envisaged that NFM may be regenerated *in situ* through a simple resintering at high temperature, which is practically relevant. SEM images in Figure 3a show the morphological evolution of the particles at three different stages, namely, freshly prepared, aged, and resintered. The fiber-like Na_2CO_3 particles disappeared after resintering, and the resintered NFM particles looked similar to the freshly prepared ones. The characteristic XRD peaks of the NFM sample became strong and sharp again after resintering, confirming that the degraded NFM returned to its original crystal structure after sintering (Figure 3b). The structural evolution during storage and resintering is also schematically summarized in Figure 3c.

We further tested the electrochemical performance of the regenerated NFM material in comparison with the freshly prepared one. Figure 4a shows the voltage curves for the freshly prepared NFM, the NFM stored for 1000 h, and the regenerated NFM. The regenerated NFM shows a specific discharge capacity of 121 mAh g^{-1}, slightly lower than that of the freshly prepared NFM (at 128 mAh g^{-1}). The difference in capacity may be attributed to the minor loss of Na due to Na_2CO_3 evaporation during the resintering, as revealed by the ICP-AES analysis (molar ratio Na/TM = 0.95 for the resintered NFM versus 0.98 for the fresh sample). The cycle performance of the regenerated NFM is compared with that of the freshly prepared one in Figure 4b, which shows a comparable cycle performance in 100 cycles by retaining ~83% of their initial capacity, respectively. The rate capability of the two samples is compared in Figure 4c (in mAh g^{-1}) and Figure 4d (in capacity retention relative to the capacity at 0.1 C). Both graphs reveal a similar trend: the discharge capacity

https://dx.doi.org/10.1021/acsaem.1c00047
ACS Appl. Energy Mater. XXXX, XXX, XXX−XXX

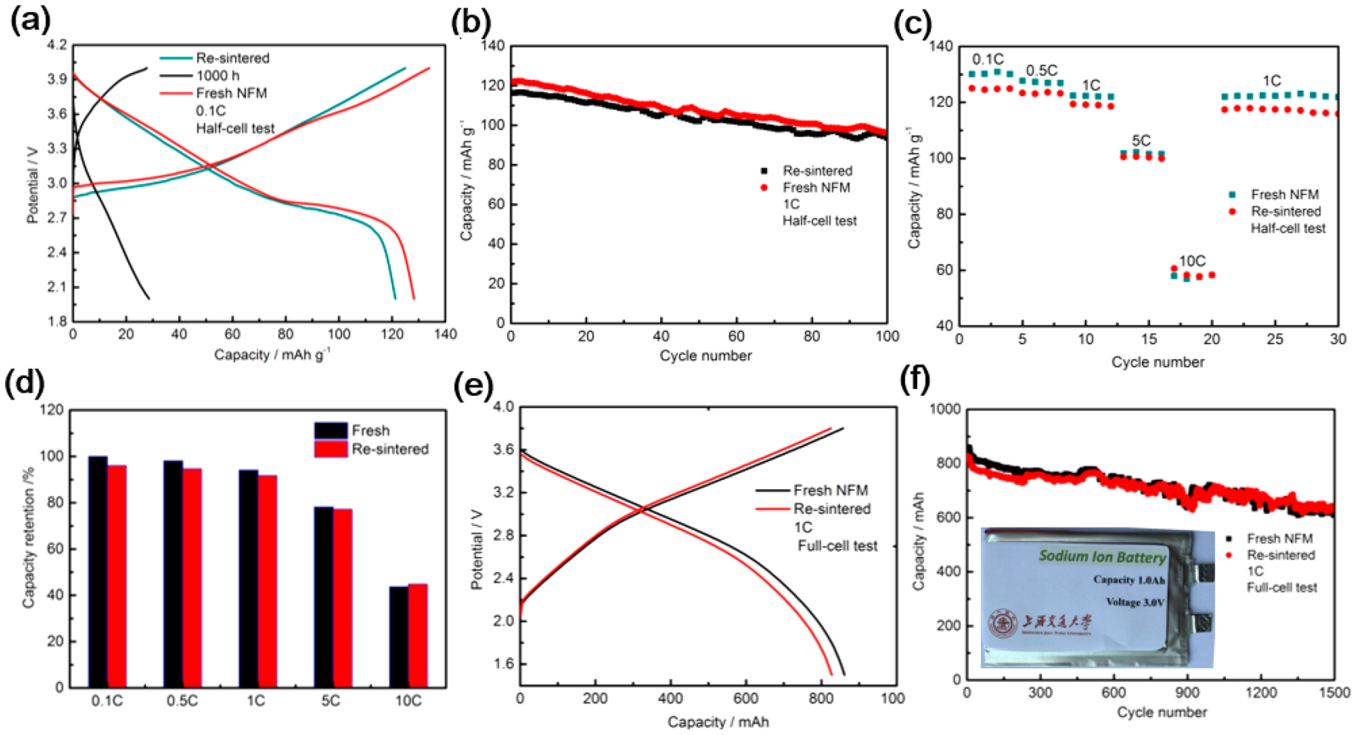


Figure 4. Electrochemical characterizations of the regenerated $NaNi_{1/3}Fe_{1/3}Mn_{1/3}O_2$. (a) The voltage profiles of the fresh, stored, and resintered NFM samples during the 1st discharge at 0.1 C. (b) Cycle performance of the three samples in half cells at 1 C between 4.0 and 2.0 V. (c, d) Rate performance of the freshly prepared and resintered NFM samples, in the unit of mAh g^{-1}, and capacity retention (%) relative to the capacity at 0.1 C, respectively. (e, f) Voltage profiles and cycle performance of the 1 Ah pouch-type full cells using the fresh and regenerated NFM as cathode and hard carbon as anode. The cycling rate is 1 C. The fluctuation in data points in panel f was caused by temperature swing in the testing room.

decreases as the current density (C-rate) increases. The rate performances for the regenerated and the fresh NFMs are comparable. The regenerated NFM shows a slightly better rate performance than the fresh one at 10 C (i.e., ~6 min charge/discharge), delivering a specific capacity of 61 versus 59 mAh g^{-1} for the fresh NFM. This may be attributed to the minor Na-deficiency in the regenerated NFM (according to ICP-AES), which improves Na^+ transport by facilitating the divacancy hopping of Na^+ ions.

The long-term cycle performance of the regenerated NFM was further evaluated for 1 Ah pouch-type full cells using hard carbon as the anode. The full cells went through a formation process at 0.1 C and were then tested galvanostatically at a current of 1 A (1 C rate) in a voltage range 3.8−1.5 V at room temperature (Figure 4e). The first-cycle discharge capacity was ~0.84 and 0.86 Ah for the regenerated NFM and the freshly prepared one, respectively. Both batteries showed excellent cycling stability and retained ~80% of the initial capacity after 1500 cycles (Figure 4f). The fluctuation in data points was caused by a temperature swing in the testing room. These results confirmed that the electrochemical performance of the aged NFM can be recovered by the resintering strategy.

In this work, we elucidated the structural and chemical degradation mechanism of an O3-type Na cathode material ($NaNi_{1/3}Fe_{1/3}Mn_{1/3}O_2$, NFM) during ambient storage. The results showed that the NFM material was reactive toward moisture and suffered from Na loss in ambient air. The lost Na migrated to the particle surface and formed fiber-like Na_2CO_3 particles as confirmed by a combination of techniques including XRD, SEM, Raman spectroscopy, and elemental analysis. These significant structural and chemical transformations were the causes of the capacity decay and the polarization increase. Furthermore, we demonstrated a simple resintering strategy to restore the structure and electrochemical properties of the NFM cathode materials. Our results highlight the importance of stringent humidity control during the material preparation and electrode fabrication processes of NFM and point to some new research directions in improving the air stability of NFM, including but not limited to surface coating (such as ZrO_2 surface modification or a hydrophobic self-assembled monolayer[30]) and doping to reduce the interlayer distance (preferentially at the surface).

■ ASSOCIATED CONTENT

Supporting Information

The Supporting Information is available free of charge at https://pubs.acs.org/doi/10.1021/acsaem.1c00047.

Experimental Methods section, and high-resolution PXRD patterns from the fresh, aged, and regenerated NFM materials (PDF)

■ AUTHOR INFORMATION

Corresponding Authors

Hong Wang − *Department of Chemical Engineering, Shanghai Electrochemical Energy Devices Research Center, Shanghai Jiao Tong University, Shanghai 200240, China*; Email: wanghnw@sjtu.edu.cn

Linsen Li − *Department of Chemical Engineering, Shanghai Electrochemical Energy Devices Research Center, Shanghai Jiao Tong University, Shanghai 200240, China*; orcid.org/0000-0002-1105-9070; Email: linsenli@sjtu.edu.cn

https://dx.doi.org/10.1021/acsaem.1c00047
ACS Appl. Energy Mater. XXXX, XXX, XXX−XXX

Zi-Feng Ma − *Department of Chemical Engineering, Shanghai Electrochemical Energy Devices Research Center, Shanghai Jiao Tong University, Shanghai 200240, China; Zhejiang NaTRIUM Energy Co. Ltd, Shaoxing 312000, China;* orcid.org/0000-0001-5002-9766; Email: zfma@sjtu.edu.cn

Authors

Yang Sun − *Department of Chemical Engineering, Shanghai Electrochemical Energy Devices Research Center, Shanghai Jiao Tong University, Shanghai 200240, China*

Dechao Meng − *Department of Chemical Engineering, Shanghai Electrochemical Energy Devices Research Center, Shanghai Jiao Tong University, Shanghai 200240, China*

Xiaoqiao Li − *Department of Chemical Engineering, Shanghai Electrochemical Energy Devices Research Center, Shanghai Jiao Tong University, Shanghai 200240, China*

Xiaozhen Liao − *Department of Chemical Engineering, Shanghai Electrochemical Energy Devices Research Center, Shanghai Jiao Tong University, Shanghai 200240, China;* orcid.org/0000-0003-4527-2424

Haiying Che − *Department of Chemical Engineering, Shanghai Electrochemical Energy Devices Research Center, Shanghai Jiao Tong University, Shanghai 200240, China; Zhejiang NaTRIUM Energy Co. Ltd, Shaoxing 312000, China*

Guijia Cui − *Department of Chemical Engineering, Shanghai Electrochemical Energy Devices Research Center, Shanghai Jiao Tong University, Shanghai 200240, China*

Fengping Yu − *Sinopec Shanghai Research Institute of Petrochemical Technology, Shanghai 201208, China*

Weimin Yang − *Sinopec Shanghai Research Institute of Petrochemical Technology, Shanghai 201208, China*

Complete contact information is available at: https://pubs.acs.org/10.1021/acsaem.1c00047

Notes

The authors declare no competing financial interest.

■ ACKNOWLEDGMENTS

This work was supported by the National Key Research and Development Program (2016YFB0901500), the Natural Science Foundation of China (21938005, 21506123, 21676165, and 22008154), the Science & Technology Commission of Shanghai Municipality (19DZ1205500), and the Zhejiang Key Research and Development Program (2020C01128).

■ REFERENCES

(1) Delmas, C. Sodium and Sodium-Ion Batteries: 50 Years of Research. *Adv. Energy Mater.* **2018**, *8*, 1703137.

(2) Hwang, J.-Y.; Myung, S.-T.; Sun, Y.-K. Sodium-Ion Batteries: Present and Future. *Chem. Soc. Rev.* **2017**, *46*, 3529.

(3) Niu, Y.-B.; Guo, Y.-J.; Yin, Y.-X.; Zhang, S.-Y.; Wang, T.; Wang, P.; Xin, S.; Guo, Y.-G. High-Efficiency Cathode Sodium Compensation for Sodium-Ion Batteries. *Adv. Mater.* **2020**, *32*, 2001419.

(4) Kubota, K.; Kumakura, S.; Yoda, Y.; Kuroki, K.; Komaba, S. Electrochemistry and Solid-State Chemistry of $NaMeO_2$ (Me = 3d Transition Metals). *Adv. Energy Mater.* **2018**, *8*, 1703415.

(5) Wang, P.-F.; You, Y.; Yin, Y.-X.; Guo, Y.-G. Layered Oxide Cathodes for Sodium-Ion Batteries: Phase Transition, Air Stability, and Performance. *Adv. Energy Mater.* **2018**, *8*, 1701912.

(6) Mu, L.; Feng, X.; Kou, R.; Zhang, Y.; Guo, H.; Tian, C.; Sun, C.-J.; Du, X.-W.; Nordlund, D.; Xin, H. L.; Lin, F. Deciphering the Cathode−Electrolyte Interfacial Chemistry in Sodium Layered Cathode Materials. *Adv. Energy Mater.* **2018**, *8*, 1801975.

(7) Wang, P.-F.; Weng, M.; Xiao, Y.; Hu, Z.; Li, Q.; Li, M.; Wang, Y.-D.; Chen, X.; Yang, X.; Wen, Y.; Yin, Y.-X.; Yu, X.; Xiao, Y.; Zheng, J.; Wan, L.-J.; Pan, F.; Guo, Y.-G. An Ordered Ni_6-Ring Superstructure Enables a Highly Stable Sodium Oxide Cathode. *Adv. Mater.* **2019**, *31*, 1903483.

(8) Pasta, M.; Wessells, C. D.; Huggins, R. A.; Cui, Y. A High-Rate and Long Cycle Life Aqueous Electrolyte Battery for Grid-Scale Energy Storage. *Nat. Commun.* **2012**, *3*, 1149.

(9) Wang, L.; Lu, Y.; Liu, J.; Xu, M.; Cheng, J.; Zhang, D.; Goodenough, J. B. A Superior Low-Cost Cathode for a Na-Ion Battery. *Angew. Chem., Int. Ed.* **2013**, *52*, 1964.

(10) Mariyappan, S.; Wang, Q.; Tarascon, J. M. Will Sodium Layered Oxides Ever Be Competitive for Sodium Ion Battery Applications? *J. Electrochem. Soc.* **2018**, *165*, A3714.

(11) Zhu, C.; Wu, C.; Chen, C.-C.; Kopold, P.; van Aken, P. A.; Maier, J.; Yu, Y. A High Power−High Energy $Na_3V_2(PO_4)_2F_3$ Sodium Cathode: Investigation of Transport Parameters, Rational Design and Realization. *Chem. Mater.* **2017**, *29*, 5207.

(12) Yao, H.-R.; Wang, P.-F.; Gong, Y.; Zhang, J.; Yu, X.; Gu, L.; OuYang, C.; Yin, Y.-X.; Hu, E.; Yang, X.-Q.; Stavitski, E.; Guo, Y.-G.; Wan, L.-J. Designing Air-Stable O3-Type Cathode Materials by Combined Structure Modulation for Na-Ion Batteries. *J. Am. Chem. Soc.* **2017**, *139*, 8440.

(13) Sun, Y.; Guo, S.; Zhou, H. Exploration of Advanced Electrode Materials for Rechargeable Sodium-Ion Batteries. *Adv. Energy Mater.* **2019**, *9*, 1800212.

(14) Vassilaras, P.; Toumar, A. J.; Ceder, G. Electrochemical Properties of $NaNi_{1/3}Co_{1/3}Fe_{1/3}O_2$ as a Cathode Material for Na-Ion Batteries. *Electrochem. Commun.* **2014**, *38*, 79.

(15) Mu, L.; Xu, S.; Li, Y.; Hu, Y.-S.; Li, H.; Chen, L.; Huang, X. Prototype Sodium-Ion Batteries Using an Air-Stable and Co/Ni-Free O3-Layered Metal Oxide Cathode. *Adv. Mater.* **2015**, *27*, 6928.

(16) Kim, D.; Lee, E.; Slater, M.; Lu, W.; Rood, S.; Johnson, C. S. Layered $Na[Ni_{1/3}Fe_{1/3}Mn_{1/3}]O_2$ Cathodes for Na-Ion Battery Application. *Electrochem. Commun.* **2012**, *18*, 66.

(17) Wang, H.; Liao, X.-Z.; Yang, Y.; Yan, X.; He, Y.-S.; Ma, Z.-F. Large-Scale Synthesis of $NaNi_{1/3}Fe_{1/3}Mn_{1/3}O_2$ as High Performance Cathode Materials for Sodium Ion Batteries. *J. Electrochem. Soc.* **2016**, *163*, A565.

(18) Xie, Y.; Wang, H.; Xu, G.; Wang, J.; Sheng, H.; Chen, Z.; Ren, Y.; Sun, C.-J.; Wen, J.; Wang, J.; Miller, D. J.; Lu, J.; Amine, K.; Ma, Z.-F. Operando XRD and TXM Study on the Metastable Structure Change of $NaNi_{1/3}Fe_{1/3}Mn_{1/3}O_2$ under Electrochemical Sodium-Ion Intercalation. *Adv. Energy Mater.* **2016**, *6*, 1601306.

(19) Xie, Y.; Xu, G.-L.; Che, H.; Wang, H.; Yang, K.; Yang, X.; Guo, F.; Ren, Y.; Chen, Z.; Amine, K.; Ma, Z.-F. Probing Thermal and Chemical Stability of $Na_xNi_{1/3}Fe_{1/3}Mn_{1/3}O_2$ Cathode Material toward Safe Sodium-Ion Batteries. *Chem. Mater.* **2018**, *30*, 4909.

(20) Che, H.; Yang, X.; Wang, H.; Liao, X.-Z.; Zhang, S. S.; Wang, C.; Ma, Z.-F. Long Cycle Life of Sodium-Ion Pouch Cell Achieved by Using Multiple Electrolyte Additives. *J. Power Sources* **2018**, *407*, 173.

(21) Che, H.; Yang, X.; Yu, Y.; Pan, C.; Wang, H.; Deng, Y.; Li, L.; Ma, Z.-F. Engineering Optimization Approach of Nonaqueous Electrolyte for Sodium Ion Battery with Long Cycle Life and Safety. *Green Energy Environ.* **2020**, available online, DOI: 10.1016/j.gee.2020.04.007.

(22) Zou, L.; He, Y.; Liu, Z.; Jia, H.; Zhu, J.; Zheng, J.; Wang, G.; Li, X.; Xiao, J.; Liu, J.; Zhang, J.-G.; Chen, G.; Wang, C. Unlocking the Passivation Nature of the Cathode−Air Interfacial Reactions in Lithium Ion Batteries. *Nat. Commun.* **2020**, *11*, 3204.

(23) Jung, R.; Morasch, R.; Karayaylali, P.; Phillips, K.; Maglia, F.; Stinner, C.; Shao-Horn, Y.; Gasteiger, H. A. Effect of Ambient Storage on the Degradation of Ni-Rich Positive Electrode Materials (NMC811) for Li-Ion Batteries. *J. Electrochem. Soc.* **2018**, *165*, A132.

(24) Zuo, W.; Qiu, J.; Liu, X.; Ren, F.; Liu, H.; He, H.; Luo, C.; Li, J.; Ortiz, G. F.; Duan, H.; Liu, J.; Wang, M.-S.; Li, Y.; Fu, R.; Yang, Y.

The Stability of P2-Layered Sodium Transition Metal Oxides in Ambient Atmospheres. *Nat. Commun.* **2020**, *11*, 3544.
(25) You, Y.; Dolocan, A.; Li, W.; Manthiram, A. Understanding the Air-Exposure Degradation Chemistry at a Nanoscale of Layered Oxide Cathodes for Sodium-Ion Batteries. *Nano Lett.* **2019**, *19*, 182.
(26) Duffort, V.; Talaie, E.; Black, R.; Nazar, L. F. Uptake of CO_2 in Layered P2-$Na_{0.67}Mn_{0.5}F_{e0.5}O_2$: Insertion of Carbonate Anions. *Chem. Mater.* **2015**, *27*, 2515.
(27) Sathiya, M.; Hemalatha, K.; Ramesha, K.; Tarascon, J. M.; Prakash, A. S. Synthesis, Structure, and Electrochemical Properties of the Layered Sodium Insertion Cathode Material: Na-$Ni_{1/3}Fe_{1/3}Mn_{1/3}O_2$. *Chem. Mater.* **2012**, *24*, 1846.
(28) Zhang, Y.; Zhang, R.; Huang, Y. Air-Stable Na_xTMO_2 Cathodes for Sodium Storage. *Front. Chem.* **2019**, *7*, 335.
(29) Li, H.; Li, J.; Ma, X.; Dahn, J. R. Synthesis of Single Crystal $LiNi_{0.6}Mn_{0.2}Co_{0.2}O_2$with Enhanced Electrochemical Performance for Lithium Ion Batteries. *J. Electrochem. Soc.* **2018**, *165*, A1038.
(30) Gu, W.; Dong, Q.; Zheng, L.; Liu, Y.; Mao, Y.; Zhao, Y.; Duan, W.; Lin, H.; Shen, Y.; Chen, L. Ambient Air Stable Ni-Rich Layered Oxides Enabled by Hydrophobic Self-Assembled Monolayer. *ACS Appl. Mater. Interfaces* **2020**, *12*, 1937.

https://dx.doi.org/10.1021/acsaem.1c00047
ACS Appl. Energy Mater. XXXX, XXX, XXX−XXX